Acta Astronautica Vol. 25, No. 11, pp. 679–686, 1991
Printed in Great Britain.

0094-5765/91 $3.00 + 0.00

MODELING AND ANALYSIS OF ORBITING TETHERS IN AN ATMOSPHERE

JORDI PUIG-SUARI and JAMES MICHAEL LONGUSKI
School of Aeronautics and Astronautics, Purdue University, West Lafayette, IN 47907, U.S.A.

(Received 21 August 1990; revised version received 26 March 1991)

Abstract—A new model for tethered satellites in low orbit, where atmospheric effects are significant, is developed. The model allows the analysis of the dynamic behavior of tethered satellites in a general orbit. The results obtained for a system in circular orbit compare favorably to previous work. The behavior of tethered systems performing aeroassisted orbital maneuvers is also simulated. In particular, the cases of elliptic orbit transfer and hyperbolic aerocapture are presented. The results in the elliptic case indicate that orbital maneuvers can be performed with small tension forces in the tether. In the hyperbolic case the behavior is not so benign, because the forces are quite large, but the utilization of tethers for aerocapture appears to be physically feasible.

1. INTRODUCTION

In recent years, with the development of new materials, the concept of long tethers in space has become feasible. Many applications for these systems have been proposed [1,2], including the deployment of tethered spacecraft in the upper atmosphere of a planet.

The analysis of a tethered satellite is very complex, more so if the effects of an atmosphere are to be taken into consideration. For this reason the early research on the subject utilizes simplifying assumptions to facilitate the understanding of the basic behavior of the system. The most common assumption is to decouple the orbital motion from the rotational motion of the spacecraft [3–5]. This assumption works very well for short tethers in circular orbit, but for long tethers the changes in attitude have a greater effect on the orbital motion. Also, if the tether is not in a circular orbit the attitude of the system is affected by the changes in position and angular velocity during the orbit. For this reason a circular orbit is also assumed in most cases [3–5]. Another common assumption is to model the tether as a rigid rod [3–5]. This assumption is reasonable in most cases, even when small aerodynamic forces are present [3], but if there are large aerodynamic forces, or if the tether undergoes large rotations this assumption must be questioned. The tether is also often assumed to be massless [4,5], which works well with short tethers, but as the tether length is increased, its mass has an increasing effect on the behavior of the system. One last assumption which is very often found in the literature is to constrain the motion of the system to the orbital plane [3,4]. For most applications this is a good approximation since the disturbances on the system in the out-of-plane direction are very small, and have little effect on the in-plane motion.

When the aerodynamic forces are included in the model, the analysis gets much more complicated. Although several applications of tethered systems in low orbit have been proposed [1–3], not much research has been done in this area.

In this paper a model for a long tethered satellite in low orbit is presented. The model takes into consideration some of the behavior that was left unexplored in earlier work. In particular, the coupling between the orbital motion and the attitude motion are taken into account. In addition, the distributed effects of drag and mass along the tether are carefully modeled. The only remaining assumptions of the literature that have been retained are rigid rod and planar motion. This improved model makes possible the study of some of the applications proposed for tethered satellites which have not yet been fully analyzed, such as aerobraking tethers.

The paper is organized in the following manner. First the new model is developed, starting from the more general assumptions just mentioned. Then the equations of motion are derived using Newton's law for the translational motion and Euler's law for the rotational motion. Next numerical results are presented and compared with some of the previous work on the subject [3] for the special case of circular orbit. New results for hyperbolic aerocapture and elliptic orbit aeroassist are also presented.

2. EQUATIONS OF MOTION

2.1. *Modeling assumptions*

The tethered system modeled in this paper, shown in Fig. 1, consists of two spacecraft, an orbiter of mass m_o and a probe of mass m_p, connected by a thin tether of length l.

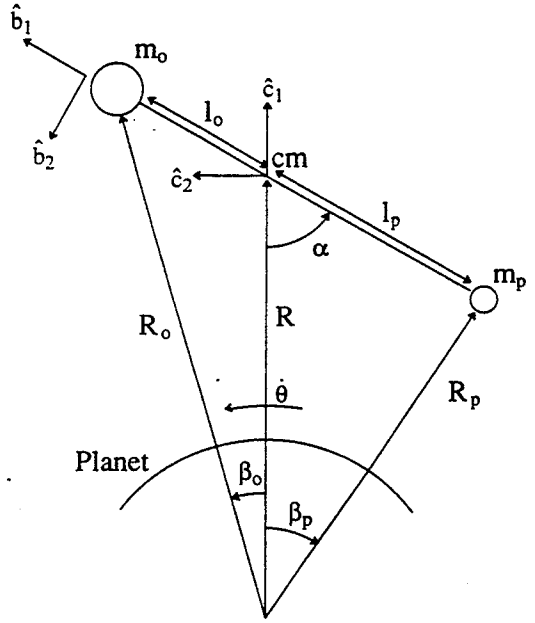

Fig. 1. Tethered system.

The system is moving in a general orbit around a rotating planet which may have a significant atmosphere. The behavior of this system is very complex. In order to simplify the analysis some assumptions are made. First, since spacecraft are usually small compared with the tethered system, the orbiter and the probe are assumed to be particles. Next the motion of the tether is constrained to the plane of the orbit. This works well in most cases since the out-of-plane disturbances are small. In addition the orbit is assumed to be equatorial and the atmosphere is assumed to rotate with the planet. Finally the tether is modeled as a rigid rod. This assumption is often made in the literature and it has proven to be reasonable in most cases [3].

These assumptions simplify the analysis significantly, but the fundamental behavior of the system is maintained. The model is general enough to allow the analysis of arbitrary initial orbits and includes the coupling between the orbital and rotational motions. The aerodynamic effect of an atmosphere is also included in order to study the behavior of tethered systems in low orbit.

The development of the equations of motion is divided into two parts. First the translational equations of motion for the center of mass of the system are developed using Newton's Law:

$$\mathbf{F} = m\mathbf{a}_{cm}. \tag{1}$$

Then the rotational equation of motion of the system about its center of mass is developed using Euler's Law:

$$\mathbf{M} = \frac{d\mathbf{H}^{cm}}{dt}. \tag{2}$$

The equations are expressed in a frame which rotates with the orbit and is represented by the vectors $\hat{\mathbf{c}}_1$ and $\hat{\mathbf{c}}_2$ in Fig. 1.

2.2. Translational equations of motion

The acceleration of the center of mass with respect to the center of the planet, which is assumed to be inertially fixed, is:

$$\mathbf{a}_{cm} = (\ddot{R} - R\dot{\theta}^2)\hat{\mathbf{c}}_1 + (R\ddot{\theta} + 2\dot{R}\dot{\theta})\hat{\mathbf{c}}_2 \tag{3}$$

where R represents the distance from the center of mass to the center of the planet and θ is the angle along the orbital path.

If the linear density of the tether is defined as η, then the total mass of the system is given by:

$$m = m_o + m_p + \eta l. \tag{4}$$

2.2.1. Gravitational forces. The gravitational forces are found assuming an inverse square model. For the two particles the forces are:

$$\mathbf{F}_{go} = -\mu m_o[(R + l_o\cos\alpha)\hat{\mathbf{c}}_1 + l_o\sin\alpha\hat{\mathbf{c}}_2]/R_o^3 \tag{5}$$

$$\mathbf{F}_{gp} = -\mu m_p[(R - l_p\cos\alpha)\hat{\mathbf{c}}_1 - l_p\sin\alpha\hat{\mathbf{c}}_2]/R_p^3 \tag{6}$$

where μ is the gravitational parameter for the planet, α represents the angular rotation of the tether with respect to the vertical direction, and l_o and l_p are the lengths along the tether from the center of mass to the orbiter and the probe respectively. R_o and R_p are the respective distances from the center of the planet and can be written as:

$$R_o = \sqrt{R^2 + l_o^2 + 2Rl_o\cos\alpha} \tag{7}$$

$$R_p = \sqrt{R^2 + l_p^2 - 2Rl_p\cos\alpha}. \tag{8}$$

Since the tether is not massless, the gravity force must be integrated along its length. This integration can be easily performed and the expression for the force acting on the tether is:

$$\mathbf{F}_{gT} = -\frac{\mu\eta}{R}\left\{\left(\frac{l_o}{R_o} + \frac{l_p}{R_p}\right)\hat{\mathbf{c}}_1 - \frac{1}{\sin\alpha}\left(\frac{R + l_o\cos\alpha}{R_o} - \frac{R - l_p\cos\alpha}{R_p}\right)\hat{\mathbf{c}}_2\right\}. \tag{9}$$

2.2.2. Drag forces. The atmospheric density of the planet, ρ_i, at radius R_i, is modeled as an exponential function:

$$\rho_i = \rho_r \exp[(H_r - R_i + R_{pl})/H] \tag{10}$$

where ρ_r is the reference density at the reference altitude H_r, H is the scale height, and R_{pl} is the radius of the planet. The atmosphere is assumed to rotate with the planet. The drag force for a body moving through an atmosphere can be written as:

$$\mathbf{F} = -\tfrac{1}{2}\rho C_D S V\mathbf{V} \tag{11}$$

where C_D is the drag coefficient, S is the frontal area of the body and $\mathbf{V}$ is its velocity with respect to the atmosphere. Using this equation, expressions for the drag forces acting on the two masses are:

$$\mathbf{F}_{Do} = -\tfrac{1}{2}\rho_o C_{Do} S_o V_o \mathbf{V}_o \tag{12}$$

$$\mathbf{F}_{Dp} = -\tfrac{1}{2}\rho_p C_{Dp} S_p V_p \mathbf{V}_p \tag{13}$$

where C_{Do} and C_{Dp} are the drag coefficients for the orbiter and the probe respectively, and S_o and S_p represent their frontal areas. Note that the masses are assumed to be spherical and the frontal area does not change with the orientation. The variables ρ_o and ρ_p represent the atmospheric density at the orbiter and probe altitudes as given in eqn (10). $\mathbf{V}_o$ and $\mathbf{V}_p$ represent the wind velocities:

$$\mathbf{V}_o = [\dot{R} - l_o(\dot{\theta} + \dot{\alpha} - \Omega)\sin\alpha]\hat{\mathbf{c}}_1 + [R(\dot{\theta} - \Omega) + l_o(\dot{\theta} + \dot{\alpha} - \Omega)\cos\alpha]\hat{\mathbf{c}}_2 \quad (14)$$

$$\mathbf{V}_p = [\dot{R} + l_p(\dot{\theta} + \dot{\alpha} - \Omega)\sin\alpha]\hat{\mathbf{c}}_1 + [R(\dot{\theta} - \Omega) - l_p(\dot{\theta} + \dot{\alpha} - \Omega)\cos\alpha]\hat{\mathbf{c}}_2 \quad (15)$$

where Ω is the angular velocity of the atmosphere. Note that the orbit is assumed to be equatorial, which means that the velocity of the atmosphere has no components perpendicular to the orbital plane. The drag force acting on the tether is found by integrating the aerodynamic effects at every point on the tether, since the density and the velocity vector change significantly along the length of the tether. The force acting on a differential tether element is given by:

$$d\mathbf{F}_{DT} = -\tfrac{1}{2}\rho_r \exp[(H_r - R_x + R_{pl})/H] \times C_{DT} V_x \mathbf{V}_x \, dS_T \quad (16)$$

where C_{DT} is the drag coefficient of the tether, assumed constant along the length, $\mathbf{V}_x$ represents the velocity, with respect to the atmosphere, of a differential portion of the tether located at a distance x from the center of mass, R_x is its distance from the center of the planet, and dS_T is the differential tether area perpendicular to the wind velocity. To simplify the integration, the tether is divided into two sections which are analyzed separately. These sections are given by l_o and l_p which are the segments of the tether above and below the center of mass, respectively (see Fig. 1). Now $\mathbf{V}_x$ and R_x can easily be written as functions of x and previously defined variables:

$$\mathbf{V}_{xo} = [\dot{R} - x(\dot{\theta} + \dot{\alpha} - \Omega)\sin\alpha]\hat{\mathbf{c}}_1 + [R(\dot{\theta} - \Omega) + x(\dot{\theta} + \dot{\alpha} - \Omega)\cos\alpha]\hat{\mathbf{c}}_2 \quad (17)$$

$$R_{xo} = \sqrt{R^2 + x^2 + 2xR\cos\alpha} \quad (18)$$

for the upper section of the tether and:

$$\mathbf{V}_{xp} = [\dot{R} + x(\dot{\theta} + \dot{\alpha} - \Omega)\sin\alpha]\hat{\mathbf{c}}_1 + [R(\dot{\theta} - \Omega) - x(\dot{\theta} + \dot{\alpha} - \Omega)\cos\alpha]\hat{\mathbf{c}}_2 \quad (19)$$

$$R_{xp} = \sqrt{R^2 + x^2 - 2xR\cos\alpha} \quad (20)$$

for the lower section. In this case the differential frontal area is not as simple as for the two masses, since its value depends on the tether orientation and the direction of the wind velocity vector at a given point on the tether. To take this effect into consideration the differential area can be written as:

$$dS_T = \frac{|\mathbf{V}_x \cdot \hat{\mathbf{b}}_2| d}{V_x} dx \quad (21)$$

where d represents the diameter of the tether, dx is a differential length along the tether, and $\hat{\mathbf{b}}_2$ is a unit vector perpendicular to the tether and aligned with $\hat{\mathbf{c}}_2$ when α is zero (see Fig. 1). To ease the integration a sign function, sgn( ), can be introduced, and assuming that there is no change in the sign of $\mathbf{V}_x \cdot \hat{\mathbf{b}}_2$ along the tether, the differential area can be written as:

$$dS_T = \mathrm{sgn}(\mathbf{V}_l \cdot \hat{\mathbf{b}}_2) \frac{\mathbf{V}_x \cdot \hat{\mathbf{b}}_2}{V_x} d \, dx \quad (22)$$

where $\mathbf{V}_l$ is the tether velocity at the end of the tether section. The case where the sign of $\mathbf{V}_x \cdot \hat{\mathbf{b}}_2$ does not remain constant can be solved by first finding the point in the tether where the sign change occurs, and then breaking the integrals into two sections corresponding to the two different signs. We call this point the *aerodynamic switching point*, because it corresponds to a position on the tether where the direction of the normal wind velocity switches. Writing $\mathbf{V}_x$, $\mathbf{V}_l$ and $\hat{\mathbf{b}}_2$ in terms of previously defined variables, the differential area expressions for each tether section become:

$$dS_{To} = \{\mathrm{sgn}[-\dot{R}\sin\alpha + R(\dot{\theta} - \Omega)\cos\alpha + l_o(\dot{\theta} + \dot{\alpha} - \Omega)] \times [-\dot{R}\sin\alpha + R(\dot{\theta} - \Omega)\cos\alpha + x(\dot{\theta} + \dot{\alpha} - \Omega)]d/V_{xo}\} \, dx \quad (23)$$

$$dS_{Tp} = \{\mathrm{sgn}[-\dot{R}\sin\alpha + R(\dot{\theta} - \Omega)\cos\alpha - l_p(\dot{\theta} + \dot{\alpha} - \Omega)] \times [-\dot{R}\sin\alpha + R(\dot{\theta} - \Omega)\cos\alpha - x(\dot{\theta} + \dot{\alpha} - \Omega)]d/V_{xp}\} \, dx \quad (24)$$

Using these expressions in the equations for the differential forces and integrating, the total drag force acting on the tether is:

$$\begin{aligned}\mathbf{F}_{DT} = {} & -\tfrac{1}{2}\rho_r C_{DT} d \exp[(H_r + R_{pl})/H] \\ & \times [\{[R(\dot{\theta} - \Omega)\cos\alpha - \dot{R}\sin\alpha] \\ & \times \dot{R}(\delta_o I_{o1} + \delta_p I_{p1}) + (\dot{\theta} + \dot{\alpha} - \Omega)[\dot{R}(1 + \sin^2\alpha) \\ & - R(\dot{\theta} - \Omega)\sin\alpha\cos\alpha] \\ & \times (\delta_o I_{o2} - \delta_p I_{p2}) - (\dot{\theta} + \dot{\alpha} - \Omega)^2 \\ & \times \sin\alpha(\delta_o I_{o3} + \delta_p I_{p3})\}\hat{\mathbf{c}}_1 + \{[R(\dot{\theta} - \Omega) \\ & \times \cos\alpha - \dot{R}\sin\alpha]R(\dot{\theta} - \Omega)(\delta_o I_{o1} + \delta_p I_{p1}) \\ & + (\dot{\theta} + \dot{\alpha} - \Omega)[R(\dot{\theta} - \Omega)(1 + \cos^2\alpha) \\ & - \dot{R}\sin\alpha\cos\alpha](\delta_o I_{o2} - \delta_p I_{p2}) \\ & + (\dot{\theta} + \dot{\alpha} - \Omega)^2\cos\alpha(\delta_o I_{o3} + \delta_p I_{p3})\}\hat{\mathbf{c}}_2] \end{aligned} \quad (25)$$

where

$$\delta_o = \mathrm{sgn}(\mathbf{V}_{lo} \cdot \hat{\mathbf{b}}_2) \quad (26)$$

$$\delta_p = \mathrm{sgn}(\mathbf{V}_{lp} \cdot \hat{\mathbf{b}}_2) \quad (27)$$

$$I_{on} = \mathrm{sgn}(l_o^* - l_o) \int_o^{l_o^*} x^{n-1} \exp(-R_{xo}/H)\,dx + \int_{l_o^*}^{l_o} x^{n-1} \exp(-R_{xo}/H)\,dx \quad (28)$$

$$I_{pn} = \mathrm{sgn}(l_p^* - l_p) \int_o^{l_p^*} x^{n-1} \exp(-R_{xp}/H)\,dx + \int_{l_p^*}^{l_p} x^{n-1} \exp(-R_{xp}/H)\,dx \quad (29)$$

where R_{xo} and R_{xp} are given in eqns (18) and (20) and where l_o^* (l_p^*) represents the aerodynamic switching point when it occurs on the orbiter (probe) side of the tether. When the switching point does not occur on the orbiter (probe) side, then $l_o^* = 0$ ($l_p^* = 0$). *Equation (25) is the exact drag force expression for the tether.* It can be combined with the expressions found previously to obtain the equations of motion for the center of mass of the system, but the integrals must be solved numerically. At this point an assumption can be made to simplify the expressions, eqns (28) and (29), and make them integrable. The problem originates from the square root terms, eqns (18) and (20). By using the approximations

$$R_{xo} = R + x\cos\alpha \quad (30)$$

$$R_{xp} = R - x\cos\alpha \quad (31)$$

and making the additional assumption that the switching point is outside of the tether (which is the usual case) then the integrals reduce to the form:

$$I_{on} = \int_o^{l_o} x^{n-1} \exp[-(R + x\cos\alpha)/H]\,dx \quad (32)$$

$$I_{pn} = \int_o^{l_p} x^{n-1} \exp[-(R - x\cos\alpha)/H]\,dx. \quad (33)$$

For $n = 1$ the integration is straightforward; for $n > 1$ the following recurrence formulas can be used:

$$I_{on} = (H/\cos\alpha)\exp(-R/H) \times \left[-l_o^{n-1} \exp(-l_o\cos\alpha/H) + (n-1) \times \int_o^{l_o} x^{n-2} \exp(-x\cos\alpha/H)\,dx \right] \quad (34)$$

$$I_{pn} = (H/\cos\alpha)\exp(-R/H)\left[l_p^{n-1} \exp(l_p\cos\alpha/H) - (n-1) \int_o^{l_p} x^{n-2} \exp(x\cos\alpha/H)\,dx \right]. \quad (35)$$

The assumption is equivalent to considering the position vectors to be parallel, so that the angles β_o and β_p are small (see Fig. 1). This approximation is valid when the tether is short, or in the case of long tethers when the orientation of the tether is close to the vertical (i.e. α is small). Finally the equations of motion for the center of mass of the system are obtained from eqns (1), (3)–(6), (9), (12), (13) and (25):

$$(m_o + m_p + \eta l)(\ddot{R} - R\dot{\theta}^2) = (\mathbf{F}_{go} + \mathbf{F}_{gp} + \mathbf{F}_{gT} + \mathbf{F}_{Do} + \mathbf{F}_{Dp} + \mathbf{F}_{DT}) \cdot \hat{\mathbf{c}}_1 \quad (36)$$

$$(m_o + m_p + \eta l)(R\ddot{\theta} + 2\dot{R}\dot{\theta}) = (\mathbf{F}_{go} + \mathbf{F}_{gp} + \mathbf{F}_{gT} + \mathbf{F}_{Do} + \mathbf{F}_{Dp} + \mathbf{F}_{DT}) \cdot \hat{\mathbf{c}}_2. \quad (37)$$

2.3. Rotational equation of motion

Since the system is assumed to move in the plane of the orbit it has only one rotational degree of freedom, therefore only one equation of motion is obtained from Euler's law.

The angular momentum of the system about its center of mass is:

$$\mathbf{H}^{cm} = [m_p l_p^2 + m_o l_o^2 + (\eta/3)(l_o^3 + l_p^3)](\dot{\alpha} + \dot{\theta})\hat{\mathbf{c}}_3 \quad (38)$$

again, written in the $\hat{\mathbf{c}}$ frame, which is moving with the orbit (see Fig. 1). The time derivative of this vector is:

$$\frac{d\mathbf{H}^{cm}}{dt} = [m_p l_p^2 + m_o l_o^2 + (\eta/3)(l_o^3 + l_p^3)](\ddot{\alpha} + \ddot{\theta})\hat{\mathbf{c}}_3. \quad (39)$$

Next the torques acting on the system about its center of mass are found. For the two masses the torques are obtained using the expressions for the forces derived in the previous section. The moments produced by the gravity forces acting on the masses are:

$$\mathbf{M}_{go} = \mu m_o R l_o \sin\alpha / R_o^3 \hat{\mathbf{c}}_3 \quad (40)$$

$$\mathbf{M}_{gp} = -\mu m_p R l_p \sin\alpha / R_p^3 \hat{\mathbf{c}}_3. \quad (41)$$

The aerodynamic forces acting on the masses yield the following moments on the system:

$$\mathbf{M}_{Do} = -\tfrac{1}{2}\rho_o C_{Do} S_o l_o V_o [R(\dot{\theta} - \Omega)\cos\alpha - \dot{R}\sin\alpha + l_o(\dot{\theta} + \dot{\alpha} - \Omega)]\hat{\mathbf{c}}_3 \quad (42)$$

$$\mathbf{M}_{Dp} = \tfrac{1}{2}\rho_p C_{Dp} S_p l_p V_p [R(\dot{\theta} - \Omega)\cos\alpha - \dot{R}\sin\alpha - l_p(\dot{\theta} + \dot{\alpha} - \Omega)]\hat{\mathbf{c}}_3. \quad (43)$$

The moments due to the tether are found by integrating along its length. For the gravity torque the integration is not difficult and gives the following expression:

$$M_{gT} = \frac{-\mu\eta}{\sin\alpha}\left[\frac{R + l_o\cos\alpha}{R_o} - \frac{R - l_p\cos\alpha}{R_p}\right]\hat{\mathbf{c}}_3. \quad (44)$$

The expression for the drag moment is more complex and it is analyzed following the same approach that was used to obtain the drag forces in the previous section. Given the differential force in eqn (16), the differential moment for a differential tether element is written as:

$$d\mathbf{M}_{xo} = x\hat{\mathbf{b}}_1 \times d\mathbf{F}_{xo} \quad (45)$$

for the upper section and:

$$d\mathbf{M}_{xp} = -x\hat{\mathbf{b}}_1 \times d\mathbf{F}_{xp} \tag{46}$$

for the lower section. These expressions can be used to obtain the following equation for the aerodynamic tether torque:

$$\begin{aligned}\mathbf{M}_{DT} = &-\tfrac{1}{2}\rho_r C_{DT} d \exp[(H_r + R_{pl})/H] \\ &\times \{[R(\dot\theta - \Omega)\cos\alpha - \dot R \sin\alpha]^2(\delta_o I_{o2} - \delta_p I_{p2}) \\ &+ 2(\dot\theta + \dot\alpha - \Omega)[R(\dot\theta - \Omega)\cos\alpha - \dot R \sin\alpha] \\ &\times (\delta_o I_{o3} + \delta_p I_{p3}) \\ &+ (\dot\theta + \dot\alpha - \Omega)^2(\delta_o I_{o4} - \delta_p I_{p4})\}\hat{\mathbf{c}}_3\end{aligned} \tag{47}$$

where, again, the integrals are given by eqns (28) and (29). The parallel vector assumption, eqns (30) and (31), permits the replacement of the integrals by the approximations in eqns (32) and (33). Now from eqns (39)–(44) and (47) the rotational equation of motion is given by:

$$\begin{aligned}&[m_p l_p^2 + m_o l_o^2 + (\eta/3)(l_o^3 + l_p^3)](\ddot\alpha + \ddot\theta) \\ &\quad = M_{go} + M_{gp} + M_{gT} + M_{Do} + M_{Dp} + M_{DT}.\end{aligned} \tag{48}$$

3. CONSTANTS OF THE MOTION

In low orbit, where the effects of an atmosphere are significant, there are no conserved quantities for the system. In the drag free case some constants of the motion exist. The analysis of these constants provides some understanding of the fundamental behavior of the system. First the total energy is known to be constant since the only force present, gravity, is conservative. The kinetic energy for the system is:

$$\begin{aligned}T = &\tfrac{1}{2}\{(m_o + m_p + \eta l)(\dot R^2 + R^2\dot\theta^2) \\ &+ [m_o l_o^2 + m_p l_p^2 + (\eta/3)(l_o^3 + l_p^3)](\dot\alpha + \dot\theta)^2\}\end{aligned} \tag{49}$$

and the gravitational potential energy is:

$$\begin{aligned}V = -\mu\left\{\frac{m_o}{R_o} + \frac{m_p}{R_p} + \eta\left[\ln\left(\frac{R_o + l_o + R\cos\alpha}{R(1+\cos\alpha)}\right)\right.\right. \\ \left.\left. + \ln\left(\frac{R_p + l_p - R\cos\alpha}{R(1-\cos\alpha)}\right)\right]\right\}.\end{aligned} \tag{50}$$

The total energy of the system is:

$$E = T + V = \text{constant}. \tag{51}$$

The kinetic and potential energies can be also used to write the Lagrangian:

$$L = T - V. \tag{52}$$

Since the Lagrangian is not a function of θ, another constant is obtained:

$$\frac{\partial L}{\partial \dot\theta} = \text{constant}. \tag{53}$$

Differentiating eqn (52), the constant is:

$$\begin{aligned}&(m_o + m_p + \eta l)R^2\dot\theta \\ &\quad + [m_o l_o^2 + m_p l_p^2 + (\eta/3)(l_o^3 + l_p^3)] \\ &\quad \times (\dot\alpha + \dot\theta) = \text{constant}\end{aligned} \tag{54}$$

which is the angular momentum with respect to the center of the planet.

4. TETHER TENSION

The tension in the tether can be easily calculated at the points where it connects with the orbiter and the probe by using Newton's law [eqn (1)]. The accelerations of the orbiter and the probe are:

$$\begin{aligned}\mathbf{a}_o = &\{\ddot R - R\dot\theta^2 - l_o[(\dot\theta + \dot\alpha)^2\cos\alpha + (\ddot\alpha + \ddot\theta)\sin\alpha]\}\hat{\mathbf{c}}_1 \\ &+ \{R\ddot\theta + 2\dot R\dot\theta + l_o[(\ddot\alpha + \ddot\theta)\cos\alpha \\ &- (\dot\theta + \dot\alpha)^2\sin\alpha]\}\hat{\mathbf{c}}_2\end{aligned} \tag{55}$$

$$\begin{aligned}\mathbf{a}_p = &\{\ddot R - R\dot\theta^2 + l_p[(\dot\theta + \dot\alpha)^2\cos\alpha + (\ddot\alpha + \ddot\theta)\sin\alpha]\}\hat{\mathbf{c}}_1 \\ &+ \{R\ddot\theta + 2\dot R\dot\theta - l_p[(\ddot\alpha + \ddot\theta)\cos\alpha \\ &- (\dot\theta + \dot\alpha)^2\sin\alpha]\}\hat{\mathbf{c}}_2.\end{aligned} \tag{56}$$

The orbiter and the probe are acted upon by aerodynamic, gravitational and tether forces. Expressions for the gravity and drag forces acting on both vehicles are given in eqns (5), (6), (12) and (13). The tether forces are the only unknowns, and can be written as:

$$\mathbf{T}_o = m_o\mathbf{a}_o - \mathbf{F}_{go} - \mathbf{F}_{Do} \tag{57}$$

for the orbiter, and:

$$\mathbf{T}_p = m_p\mathbf{a}_p - \mathbf{F}_{gp} - \mathbf{F}_{Dp} \tag{58}$$

for the probe. These equations are written in the $\hat{\mathbf{c}}$ vector frame. To analyze tether tension it is more convenient to utilize the $\hat{\mathbf{b}}$ frame, which is fixed in the tether (see Fig. 1). The vector transformation is:

$$\begin{aligned}\mathbf{T} = &[(\mathbf{T}\cdot\hat{\mathbf{c}}_1)\cos\alpha + (\mathbf{T}\cdot\hat{\mathbf{c}}_2)\sin\alpha]\hat{\mathbf{b}}_1 \\ &+ [-(\mathbf{T}\cdot\hat{\mathbf{c}}_1)\sin\alpha + (\mathbf{T}\cdot\hat{\mathbf{c}}_2)\cos\alpha]\hat{\mathbf{b}}_2.\end{aligned} \tag{59}$$

Note that the $\hat{\mathbf{b}}_2$ component of the force, perpendicular to the tether, is nonzero in general because the tether is assumed to be a rigid rod. This component of the tether force provides an indication of the accuracy of the rigid rod approximation. The $\hat{\mathbf{b}}_1$ component, directed along the tether, can be positive or negative since a rod can be loaded in compression as well as in tension. The presence of compressive forces is unacceptable for a tethered system, and care must be taken to ensure that they are never encountered in the proposed applications.

5. EQUILIBRIUM POSITIONS

In this section we analyze equilibrium positions where the angle α, which represents the tether orientation, is constant. The behavior of α is given by the rotational equation of motion [eqn (48)]. The left-

hand side of the equation shows a direct relation between the changes in θ and α. Recall that θ represents the orbital angular position. This relationship makes it impossible to have equilibrium conditions in orbits where the changes in θ are not equal to zero, which means that *equilibrium can only be found in circular orbits*. Note that the relation between the behavior of the two angles also implies that the orbital motion is directly affected by the satellite motion; therefore, if the tether is not in equilibrium a perfectly circular orbit can not be maintained.

For a circular orbit, $\dot{\theta}$ can be eliminated from the equation. At this point, the equilibrium condition is found by setting the right-hand side of eqn (48) equal to zero. This gives the tether orientation where the sum of the moments acting on the system is equal to zero. If the aerodynamic effects are ignored, then two equilibrium orientations are found. First, a stable one is easily found for α equal to zero (in the limit). The second one is unstable, and it is located at α equal to $\pi/2$ when the masses of the orbiter and the probe are equal. The unstable equilibrium position moves away from the value of $\pi/2$ as the mass ratio of the two vehicles changes, and numerical techniques must be utilized to solve for the position since the equation becomes transcendental. (Note that the change in mass ratio moves the position of the center of mass away from the geometric center of the tether, and that the angle α is measured with respect to the position vector to the center of mass.) When the drag effects are included two solutions are also possible if the assumption of circular orbit is maintained. For small aerodynamic effects the equilibrium positions are close to those found in the drag free case. The differences increase as the aerodynamic torques become more significant. The stability of these orientations is similar to that of the drag free cases, with the attitude close to zero being stable and the one close to $\pi/2$ being unstable. For all mass ratios the equation is transcendental when the drag torques are included and both positions must be obtained utilizing numerical methods. Note that to maintain circular orbit, necessary for the equilibrium conditions, thrust must be applied to the system to cancel the drag forces. (Otherwise, the orbit would decay.)

6. NUMERICAL RESULTS

In this section the equations obtained previously are utilized to numerically simulate various tethered systems in orbit about Mars including the cases of circular orbit, elliptic orbit and hyperbolic aerocapture. In these examples the radius of Mars is assumed to be 3398 km and the gravitational constant is $4.28 \times 10^4\ km^3/s^2$.

6.1. Circular orbit

An analysis of a tethered system for the exploration of the planet Mars is found in [3] and has provided a source of inspiration to the authors. The system consists of an orbiter and a probe connected by a long thin tether. The probe is low enough to make the aerodynamic effects on the system significant. The model in [3] is limited to the case of a spacecraft maintained in circular orbit by continuous thrust. As discussed earlier, an equilibrium position for this system is possible. The new model presented above is generally applicable to all types of orbits and so includes this special case as a subset. It is interesting to compare the results of [3] with the new model.

Table 1. Tethered system parameters

Orbiter mass	1000 kg
Orbiter C_{Do}	2
Orbiter frontal area	10 m^2
Probe mass	500 kg
Probe C_{Dp}	1
Probe frontal area	1 m^2
Tether linear density	0.3 kg/km
Tether C_{DT}	2
Tether diameter	0.5 mm

6.1.1. Thrusting case. The input values given in Table 1 are taken from the analysis in [3]. These values provide the physical characteristics of the system. Several cases are studied utilizing different tether lengths and orbit radii. Using these data the equilibrium position can be found numerically, and represents the tether orientation where the torques acting on the system cancel. Note that the analysis includes a thrust force acting on the orbiter that cancels all forces except the radial component of gravity. Once the equilibrium orientation is found, values for all forces and moments present are also available. The dynamic behavior of the system can also be simulated and it is found that, as expected, the system maintains the same orientation for all time. The results obtained with the new model are shown in Table 2, and are similar to those found in [3].

The differences are due to the fact that the model in [3] included some additional simplifying assumptions such as constant velocity along the tether and parallel position vectors. This last assumption eliminates gravity forces in the $\hat{\mathbf{e}}_2$ direction, which can be of the order of 10 N in some cases, and also eliminates drag forces in the $\hat{\mathbf{e}}_1$ direction. Both of these forces affect the value and direction of the thrust required to maintain circular orbit. Overall, the two models are in agreement about the behavior of the system. Note that the new model is not restricted to the study of systems in equilibrium. The dynamic behavior of tethered spacecraft with no thrust available or initially placed at nonequilibrium positions can also be analyzed, as shown in the next subsections.

Table 2. Equilibrium conditions in circular orbit

Tether length (km)	Orbit radius (c.m.) (km)	Equilibrium α (deg)
190	3634	0.665
200	3630	2.314
212	3627	7.377
243	3623	24.670
296	3621	40.005

6.1.2. Non-thrusting case. The case of a spacecraft initially placed in a circular orbit at the equilibrium position but with no thrust available is discussed next. This case demonstrates the possibility of using the new model to analyze systems with complicated behavior, where there is a strong coupling between the orbital motion and the tether orientation. This coupling is due to the fact that the orbital motion is continuously changed by the drag forces which are determined by the altitude of the orbit and the attitude of the tether. The input values are again taken from the analysis in [3], in particular the case where the tether length is 212 km. For the initial orbit the equilibrium angle is found to be 5.33°. Note that it is different than before since no thrust forces (nor their associated torques) are present in this case. The dynamic behavior of the system is shown in Fig. 2. The results clearly show the changes in the tether orientation and the orbit decay caused by the drag forces.

Of course it is not necessary to permit the tether system to go through the entire orbit decay process. The probe can be pulled out of the atmosphere by reeling in the tether, eliminating the drag forces that affect the orbit. Also the tether can be cut, sending the probe into a landing trajectory while boosting the orbiter into a higher orbit away from the atmosphere.

6.2. Elliptic orbit

An aerobraking tether can be used to reduce the eccentricity of a spacecraft in an elliptical orbit. The aeroassist maneuver is performed by dropping a probe, connected to the spacecraft by a long tether, into the upper atmosphere of the planet. In this approach only the probe travels through the atmosphere, eliminating the aerodynamic requirements (such as heat shielding and aerodynamic streamlining) on the orbiter. Large changes to the orbit are possible with one pass through the atmosphere, but the material strength requirements on the tether may be extreme. The loads on the tether are largely reduced if the maneuver is performed in several passes. A simulation of one such pass is shown in Fig. 3. The spacecraft studied is the one used in the circular orbit case with a tether length of 260 km. The

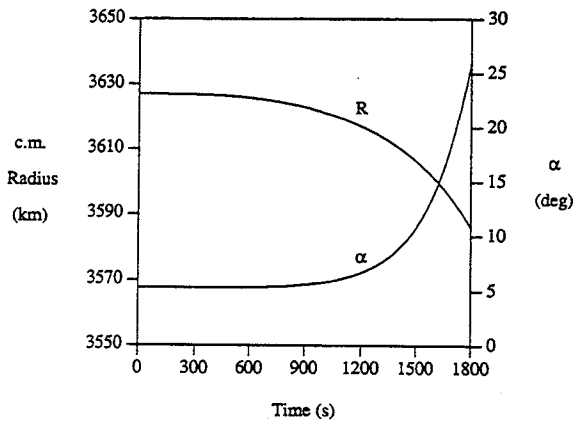

Fig. 2. Non-thrusting case.

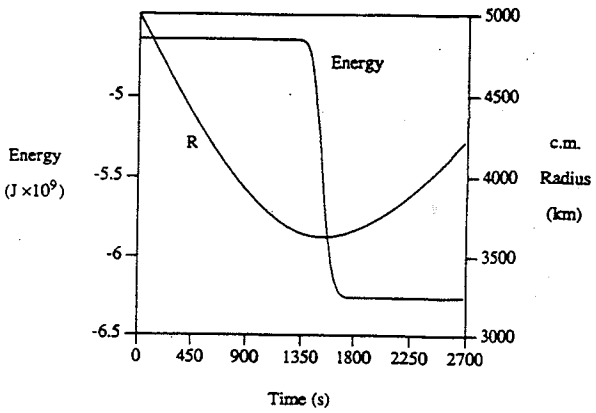

Fig. 3. Elliptic transfer.

spacecraft is initially placed in an elliptic orbit with eccentricity 0.5 and semimajor axis 7250 km (assuming the tether is a point mass). The simulation starts with the spacecraft placed away from the atmosphere and with an attitude that places the probe in the atmosphere at periapsis, where the braking maneuver takes place. The results, given in Fig. 3, show the effect of the aerodynamic drag on the orbit. During the maneuver the minimum altitude reached by the probe is 58 km, while the orbiter maintains an altitude of over 300 km. The forces found in the tether have a maximum value of approx. 1500 N. This value exceeds the strength of the tether described in [3], but is acceptable given the strength of currently available materials. These results are very encouraging and open the way to the development of a new type of spacecraft to be used in planetary exploration. The probe may be equipped with sensors for atmospheric studies or may even be designed to land on the planet after the maneuver is completed. This allows the probe to provide scientific data at the same time that the aerobraking eliminates a propulsive maneuver.

It should be noted, however, that the rigid rod approximation presents some modeling problems since the simulation indicates that a large normal component of force acts on the tether. The maximum angle between the tether and the force vector is close to 80°. This result is inconsistent with the flexible behavior characteristic of a thin tether. On the other hand, the results of the flexible tether analysis in [3] show that it is possible to have transverse force components at the extremes of the tether while most of it remains straight. The analysis must eventually be extended to the case of a flexible tether, but these preliminary results are very positive.

6.3. Hyperbolic orbit

The utilization of aerobraking tethers for aerocapture presents some advantages over conventional vehicles. The orbiter is maintained in a high orbital path away from the atmosphere, which eliminates the need for thermal protection in the orbiter. The drag acting on the probe serves a double purpose. First it slows the entire system to place it in orbit around the

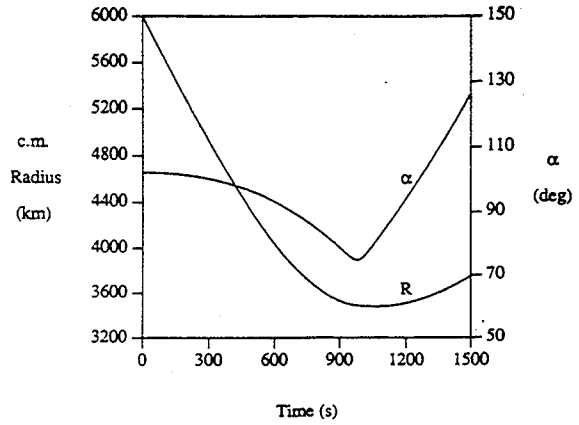

Fig. 4. Hyperbolic aerocapture.

planet. Second, after severing the tether, the probe can be delivered to the surface of the planet. The significant advantage of this system is that no propulsive braking maneuver is required. In addition, a long tether may avoid the sensitivity problems of conventional aerocapture [6]. If the tether is cut, the well-known tendency of the probe to drop into a lower orbit while the orbiter rises to a higher orbit can be a useful advantage. The aerobraking problem is simulated using the parameters of Table 1 with a tether length of 290 km. The hyperbolic orbit is chosen to represent a general Earth to Mars transfer (eccentricity 2.0 and semimajor axis −3485 km). The initial radius is taken far away from the planet where atmospheric effects are not present. The initial tether orientation is chosen so that the natural motion of the system places the probe at a low altitude during periapsis, where the drag effects are significant. The energies of the system and of the individual particles (the probe and the orbiter) are monitored to determine the point at which aerocapture is achieved. The behavior of the system is shown in Fig. 4, where dramatic changes in R and α occur at the time when the energy of the system becomes negative (at approx. 1000 s). During the maneuver the orbiter reaches a minimum altitude of 97 km while the probe descends to an altitude of 45 km. *These results indicate that aerocapture can be achieved while maintaining the orbiter away from the sensible atmosphere.*

This possibility leads to some exciting implications that may have significance in future space vehicles. However some problems remain unsolved. Very large tension forces, up to 20,000 N, are present. This indicates that a strong tether is required, and with present materials this implies great mass. Alternatively, new materials may provide greater strength. The forces also indicate that, as in the elliptic transfer case, the rigid rod model is not entirely valid since some transverse components and even compressive components are found in the rigid tether. As mentioned before, the flexible tether analysis in [3] indicates that the rigid tether model may be a good approximation even in cases where the tether forces at the masses are not consistent with a flexible tether. Eventually the effects of flexibility must be included in the analysis, but these initial results indicate that aerocapture with tethers is possible.

7. CONCLUSIONS

The results obtained with the new tether model indicate that the use of tethers in an atmosphere is feasible for circular and elliptic orbits. For aerocapture from hyperbolic orbit, the forces are very large, but the behavior of the system is quite acceptable in that the orbiter is maintained at a safe altitude throughout the aerobraking maneuver. The large forces are of course closely tied to the physical parameters of the particular problem studied here.

REFERENCES

1. J. A. Carroll, Tether applications in space transportation. *Acta Astronautica* **13**, 165–174 (1986).
2. *Tethers in Space Hand Book*. Office of Space Flight Advanced Programs (NASA), Washington (1986).
3. E. C. Lorenzini, M. D. Grossi and M. Cosmo, Low altitude tethered Mars probe. *Acta Astronautica* **21**, 1–12 (1990).
4. J. V. Breakwell and J. W. Gearhart, Pumping a tethered configuration to boost its orbit around an oblate planet. *J. Astronaut. Sci.* **35**, 19–40 (1987).
5. D. A. Arnold, The behavior of long tethers in space. *J. Astronaut. Sci.* **35**, 3–18 (1987).
6. N. X. Vinh, J. R. Johannesen, J. M. Longuski and J. M. Hanson, Second-order analytic solutions for aerocapture and ballistic fly-through trajectories. *J. Astronaut. Sci.* **32**, 429–445 (1984).